Direct probe of oxygen superstructures in manganites

Stéphane Grenier, K. J. Thomas, J.P. Hill, U. Staub, Y. Bodenthin, M. Garcia-Fernandez, V. Scagnoli, V. Kiryukhin, S.-W. Cheong, B. G. Kim, et al.

▶ **To cite this version:**

Stéphane Grenier, K. J. Thomas, J.P. Hill, U. Staub, Y. Bodenthin, et al.. Direct probe of oxygen superstructures in manganites. 2007. hal-00149105v1

HAL Id: hal-00149105
https://hal.science/hal-00149105v1

Preprint submitted on 24 May 2007 (v1), last revised 16 Nov 2007 (v2)

HAL is a multi-disciplinary open access archive for the deposit and dissemination of scientific research documents, whether they are published or not. The documents may come from teaching and research institutions in France or abroad, or from public or private research centers.

L'archive ouverte pluridisciplinaire **HAL**, est destinée au dépôt et à la diffusion de documents scientifiques de niveau recherche, publiés ou non, émanant des établissements d'enseignement et de recherche français ou étrangers, des laboratoires publics ou privés.

Direct probe of oxygen superstructures in manganites

S. Grenier,[1] K. J. Thomas,[2] J. P. Hill,[2] U. Staub,[3] Y. Bodenthin,[3] M. García-Fernández,[3] V. Scagnoli,[4] V. Kiryukhin,[5] S-W. Cheong,[5] B. G. Kim,[5,*] and J. M. Tonnerre[1]

[1]*Institut Néel, CNRS & Université Joseph Fourier, BP 166, F-38042 Grenoble Cedex 9, France*
[2]*Condensed Matter Physics and Materials Science Dept., Brookhaven National Laboratory, Upton, New York 11973, USA*
[3]*Swiss Light Source, Paul Sherrer Institut, 5232 Villigen, Switzerland*
[4]*European Synchrotron Radiation Facility, BP 220, F-38043 Grenoble Cedex 9, France*
[5]*Department of Physics and Astronomy, Rutgers University, Piscataway, New Jersey 08854 USA*

(Dated: May 24, 2007)

We report the observation of superstructures associated with the oxygen $2p$-states in two prototypical manganites using x-ray diffraction at the oxygen K-edge. We determine the nature of the orderings and discuss our picture with respect to novel theoretical models. In $Bi_{0.31}Ca_{0.69}MnO_3$, hole-doped O states are found to be orbitally ordered, at the same propagation vector as the Mn orbital ordering, but no evidence is found to support a picture of oxygen stripes at this periodicity. In $La_{\frac{7}{8}}Sr_{\frac{1}{8}}MnO_3$, we observe a $2p$ charge ordering described by alternating hole-poor and hole-rich MnO planes that is consistent with recent predictions.

Fascinating macroscopic properties may emerge from the electronic and magnetic orderings that occur in $3d$ metal oxides doped with charge carriers. In doped cuprates, charge and spin stripes could be relevant to high-T_C superconductivity [1], and the colossal magnetoresistance of doped manganites is fundamentally related to the stability, in a magnetic field, of an ordering of polarons together with an ordering of charge, orbital and magnetic moments on the Mn atoms [2]. The relationship between the orderings and the transport properties has been adressed both theoretically and experimentally concentrating on the $3d$ metal atoms, often neglecting the ligands' degrees of freedom. The active states are not ionic $3d$ metal orbitals however, but, rather hybridized metal $3d$ - oxygen $2p$ states; therefore, an ordering of the metals is concomittant with an ordering of the oxygens. In cuprates, the role of the oxygen atom is now always considered and, taking a recent example, the ordering of hole-doped oxygens was directly observed and discussed in the context of the stripes [3].

In manganites, an electronic ordering on oxygens has not been detected yet although recent experiments suggested a crucial role of the O atoms in the polaronic, electronic, and magnetic orderings of the Mn atoms. A relation between conductivity and the O electronic configuration has been identified [4]. Also, spectroscopic studies have indicated a small charge disproportionation on Mn atoms instead of an ionic charge ordering (Mn^{4+}/Mn^{3+}) [5], and thereafter, a crystallographic study proposed that the oxygen atom bridges an electron between two Mn atoms of nearly the same valence, coupling them magnetically [6]. At the heart of these results is the explicit role of the $2p-3d$ hybridization in determining the magnetic exchange couplings and conductivity, the traditional picture being the one where the atomic $3d$ orbitals define exchange magnetic pathways between Mn atoms, the oxygen $2p$ states being filled.

Meanwhile, new theoretical models beyond the Mn-centered description have also suggested that oxygen superstructures play an important role in determining the ground states of manganites. With *ab initio* calculations, Ferrari *et al.* [7] explained the insulating behavior of the charge/orbitally orded half-doped system by an ordering of O holes - "oxygen stripes" of varying valences (incidentally, having the same periodicity as the Mn orbital ordering). Similarly, Efremov *et al.* [8] proposed that the charge ordering could correspond to a charge density wave (CDW) that is either Mn-centered or O-centered; they then show that an intermediate CDW (an intermediate O-Mn charge transfer) would potentially give both ferromagnetism and ferroelectricity. Finally, Volja *et al.* [9] insisted on the relevance of the Mn charge ordering concept, if the hybridization with the hole-doped oxygen atoms is properly considered.

Experiments that directly probe the oxygen contribution to the ordered states provide essential feedback to these theoretical models. In this Letter, we present the O K-edge resonant diffraction spectra that reveal the oxygen superstructures in two manganites. We first report the direct observation of the *orbital* ordering of hole-doped, hybridized, O $2p$-states in a Mn-centered, Mn-orbitally ordered manganite, $Bi_{1-x}Ca_xMnO_3$ ($x = 0.69$). Second, we report the *charge* ordering on the oxygen in $La_{\frac{7}{8}}Sr_{\frac{1}{8}}MnO_3$; our observations confirm the stacking of alternate hole-rich and hole-poor planes. In both cases, the O states are directly related to the Mn states, emphasizing the hybridized nature of the active states involved in the electronic orderings.

$Bi_{0.31}Ca_{0.69}MnO_3$ (BCMO) is representative of the Mn-centered orbitally ordered CDW phase. This phase is robust in manganites, over a wide doping range, from half-doping to at least $x = 0.8$ [2]. The CDW exhibits polaronic sites (Mn^{3+}) placed as far as possible from each other, with an antiferro order of the valence orbital, while

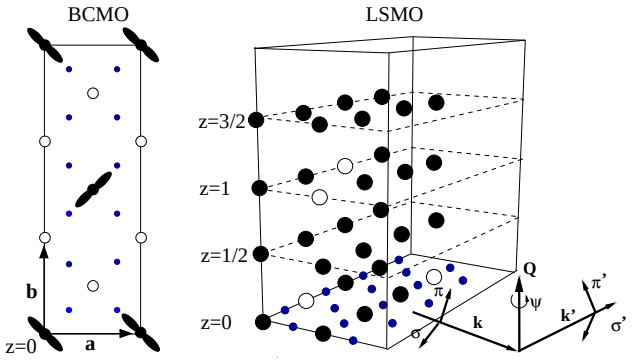

FIG. 1: Simplified orderings in BCMO and LSMO. Closed circles represents polaronic Mn^{3+} atoms, open circle are Mn^{4+} and small circles are the oxygen sites; the orbital ordering in BCMO is also shown. The structure in the a-b plane of BCMO repeats in adjacent planes, while LSMO planes alternate between being hole-rich (z=0 and 1) and hole-poor (z=1/2 and 3/2) [11]; for clarity the oxygens are represented in the first plane only. The scattering geometry is indicated, ψ is the azimuthal angle, σ and π are the two polarization components.

Mn^{4+} sites are isotropic [10] (see Fig. 1). As the doping increases, the polaron density diminishes, and a larger orbital ordering periodicity is obtained ($\Lambda \approx 17$ Å for BCMO), which is large enough to diffract soft x-rays near the O K-edge ($\lambda = 23.4$ Å at 530 eV). BCMO orders below $T_{OO} = 250$ K. The second system, $La_{\frac{7}{8}}Sr_{\frac{1}{8}}MnO_3$ (LSMO), exhibits several phase transitions upon cooling. At $T_{OO1} \approx 280$ K, a polaronic insulating orbital ordering takes place. Then, the system becomes a metallic ferromagnet at $T_C \approx 180$ K and finally stabilizes below $T_{OO2} \approx 150$ K as an insulating ferromagnet. It was recently demonstrated that the OO1 to OO2 transition corresponds to a rearrangement of the polarons in a larger unit cell [11]. Here, we directly probed the electronic ordering that underlies the polaron rearrangement, which allowed us to confront two recent models for the electronic structures (described below).

The BCMO compound was prepared by the flux technique and LSMO by the floating zone technique; both samples were characterized by hard x-ray diffraction. The crystals were cut and polished with the normal to the surface along [010] for BCMO, and along [001] for LSMO. We refer to the Pbnm orthorhombic notations for the unit cell.

The RXD data were collected at the SIM beamline of the Swiss Light Source using the RESOXS chamber [12]. The experiments were performed as in conventional diffraction but with the incident energy varied through the O K-edge whilst moving the diffractometer angles to maintain the diffraction condition. The O K-edge corresponds to the photoelectric transition of a 1s electron to unoccupied orbitals ψ_n. This resonant process is accounted for in the scattering factor by the overlap integral $\hat{\varepsilon} \cdot \int \psi_n(\mathbf{r}) \mathbf{r} \psi^{\mathrm{O}}_{1s}(\mathbf{r}) d\mathbf{r}$; the resonant factor and the Thomson scattering factor are then weighted by the crystallographic phase-factor at the selected Bragg reflection, $F(Q,\omega) = \sum_j f_j(Q,\omega) e^{i\mathbf{Q}\cdot\mathbf{r}_j}$, $\hat{\varepsilon}$ being the photon polarization, and ω the energy of the photon and the energy between ψ_n and ψ^{O}_{1s} [13]. The resonant reflection provides evidence of the periodicity of near-ε_f states, and sweeping the incident photon energy through the O K-edge, therefore effectively probes the spectrum of unoccupied states ψ_n from and above ε_f at this periodicity. We note that the unoccupied orbitals probed must not have an even symmetry relatively to the oxygen 1s orbital ψ^{O}_{1s} (which is even), as easily seen from the overlap integral expression. Near the Fermi level (ε_f), those may be O 2p's, or orbitals from nearby atoms with some projection on the oxygens (*e.g.* 3d), or orbitals made of a hybridization of the two. We also measured azimuthal scans (record of the reflection intensity while rotating the crystal in a plane normal to $\mathbf{Q}$) which allow one to rotate the polarization of the photon relatively to the crystal thereby probing different directions of the unoccupied states (ψ_{2p_x},...). We could select the two incident polarizations, namely σ or π, perpendicular to and within the scattering plane, respectively (Fig. 1), but there is no polarization analysis at the detector.

Fig. 2a shows the O K-edge RXD spectrum at the (0 0.31 0) superstructure reflection we found in BCMO, for π and σ incident polarizations. No scattering is observed outside a narrow energy range (1.1 eV) at the edge of the absorption spectrum (given by the fluorescence yield). A second observation is the equal scattering amplitude for the two incident polarizations. As has been discussed elsewhere [10] this implies that the scattering process is one in which the polarization of the photon is rotated, of the type $\sigma \rightarrow \pi$ or $\pi \rightarrow \sigma$, that is, with zero $\sigma \rightarrow \sigma$ and $\pi \rightarrow \pi$ scattering. The incommensurability of this reflection is observed to vary with temperature, stabilizing at about 0.31 r.l.u., below T_{OO} (Fig. 2b). A final observation, from Fig. 2c, is the extinction of the reflection when the polarization of the incident photon is perpendicular to the ordered (a,b) plane.

The first observation indicates a resonant superstructure reflection from an ordering of the very first unoccupied states from ε_f projected on the oxygen atoms (ψ^O_{1s}), with the propagation $Q = 0.31$ r.l.u, corresponding to the periodicity of the Mn orbital ordering [10]. Following earlier analysis of the absorption data [14], the comparison with the fluorescence yield allows us to identify the ordered states as the 2p states hybridized with the 3d. The narrow spectral width observed reflects the width of this hybridized band. The second observation demonstrates that there is no charge ordering on oxygen atoms *at this wave vector*. Indeed, a CDW of this periodicity would scatter in the $\sigma \rightarrow \sigma$ channels, which is absent on this reflection to within the uncertainty of our measurements. Furthermore, a charge order scatters at all azimuthal an-

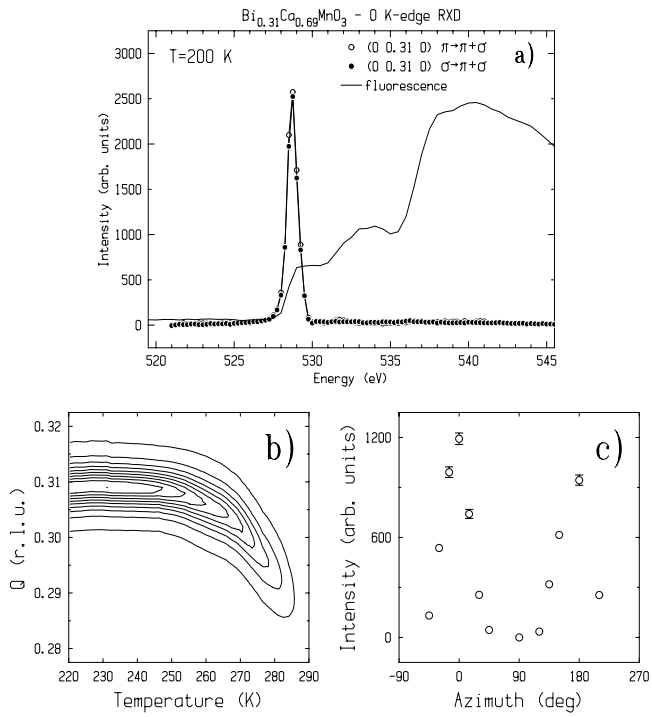

FIG. 2: a) The (0 0.31 0) superstructure reflection, corrected from fluorescence but not for self-absorption; nevertheless, the intensity is zero off the O K-edge. b) Temperature dependence of the peak position at the phase transition. c) Azimuthal dependence displaying a two-fold symmetry with a maximum with the incident polarization along **a**, and zero along **c**, taken at 528.75 eV, T=200K.

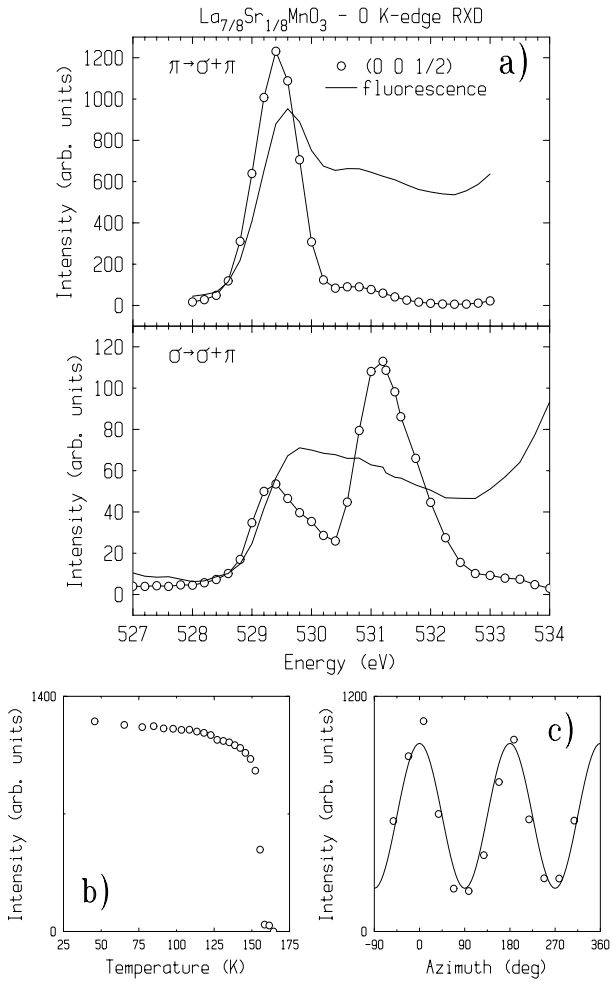

FIG. 3: a) RXD spectra of the $(00\frac{1}{2})$ reflection at the O K-edge of $La_{\frac{7}{8}}Sr_{\frac{1}{8}}MnO_3$, with two incident polarizations, $T = 30$ K. The spectra were obtained after a fit to the reflection with a square Lorentzian, providing the intensity of the reflection and the fluorescence yield from the background. b) Temperature dependence of the reflection. c) Azimuthal dependence at 529.2 eV, $\sigma \rightarrow \sigma + \pi$ channels, compared to a $\cos^2 + cst$ function (solid line), 0 deg. corresponds to the σ incident polarization along **b**, 90 deg. along **a**.

gles [15, 16], at odds with the observation of zeros of the signal. These three observations prove that the O $2p$ states are hole-doped and show orbital ordering, and not charge ordering at this propagation vector. Therefore, the data exclude a direct extension to this high doping of the model of oxygen stripes at the periodicity of the Mn orbital ordering [7].

The observation of $2p$ orbital ordering makes intuitive sense in light of the $2p-3d$ hybridization and the earlier observation of this same orbital ordering, but projected on the Mn atoms (ψ_{2p}), at the Mn $2p \leftrightarrow 3d$ L-edge [10]. Specifically, these states are centered on the polaronic Mn atoms, with a configuration depicted in Ref. [9, 17] clearly exhibiting the unoccupied $2p$ ordering on the four oxygens surrounding the polaronic Mn. In regard of these latter models, the charge transfer nature of the compound, the hybridization, thus the relation with the Mn orbital ordering, are evident from our results.

We now turn to $La_{\frac{7}{8}}Sr_{\frac{1}{8}}MnO_3$. Fig. 3a shows the RXD spectra of the $(00\frac{1}{2})$ superstructure reflection at the O K-edge for two incident polarizations. Previous studies have already reported the unusual stacking that doubles the unit cell along **c** below T_{OO2} [18]; the present data also reveals a specific $2p$-state reordering (Fig. 3a and b). The fluorescence yields are observed to be different for the two polarizations at the edge, the differences providing evidence of an anisotropy of the unoccupied O-states near ε_f. The main characteristic of the $2p$ ordering is identified by considering the azimuthal dependence of the reflection. The azimuthal scan never goes to zero; it has a near perfect $\cos^2 +$ const dependence (Fig. 3c). A tensorial analysis of the resonant scattering permits to easily identify the origin of the two terms [16]: The constant term is due to a net difference in the total charge carried by the oxygens on different planes, whereas the sinusoidal dependence is due to the relative direction of the polarization of the photon with the anisotropic O electronic structure.

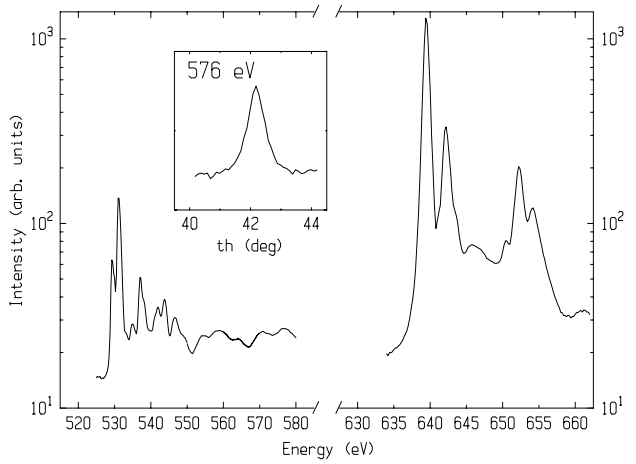

FIG. 4: Resonant diffraction spectrum of the $(00\frac{1}{2})$ reflection at the O K-edge and Mn L-edges of $La_{\frac{7}{8}}Sr_{\frac{1}{8}}MnO_3$, $\sigma \rightarrow \sigma + \pi$ channels, $T = 30$ K. Three distinctive regions should be considered. The amplitude at the O K-edge and Mn L-edges is a probe of the states near ε_f, projected on O and Mn atoms respectively. The amplitude between 535 and 560 eV is mostly unsensitive to the active states, but reflects the positions of neighboring atoms due to band structure effects. Inset is the profile of the reflection at 576 eV.

The diffraction vector $(0\ 0\ \frac{1}{2})$ corresponds to the net difference in scattering, hence to a net difference in holes, from planes separated by $\Delta z = 1$; a charge ordering at the $(0\ 0\ \frac{1}{2})$ vector provides a strong constraint to the theoretical models. The models by Korotin *et al.* [19] and by Geck *et al.* [11] both propose that hole-rich and hole-poor Mn planes alternates along **c**, but with different stacking orders. In Geck's model every other planes are identical when projected on the **c** axis: they should not give the charge order scattering we observe. In Korotin's model however, three successive hole-poor planes alternate with one hole-rich plane. Such order should give rise to a strong charge order signal on the O atoms because of the hybridization, as we observe. We note that only Geck's model explains reflections with a planar component observed elsewhere [11], but the ordering of the holes along **c** is not consistent with our data.

Finally, we also report on the scattering observed at this wave-vector for energies well above the O K-edge (Fig. 4). This scattering probes the np continuum that is sensitive to the local atomic configuration due to band structure effects. These features signal the necessary lattice distortions to accomodate the charge ordering. Increasing again the photon energy, it was natural to look also for the signal at the Mn L-edge which is again a direct probe of the states nearby ε_f, but projected on the Mn atoms (Fig. 4). Correspondingly, the data are direct observation of differing Mn $3d$ configurations; this will be discussed in detail elsewhere.

In conclusion, resonant x-ray diffraction at the O K-edge has been used to detect the electronic superstructures of the $2p$ states near ε_f in two manganites. In $Bi_{0.31}Ca_{0.69}MnO_3$, we show evidence of an orbital ordering of hole-doped hybridized $2p-3d$, and contradict oxygen stripes with the same propagation vector as the Mn orbital ordering. In $La_{\frac{7}{8}}Sr_{\frac{1}{8}}MnO_3$, the data provided the evidence of a charge ordering on the oxygen atoms with the unusual $(0\ 0\ \frac{1}{2})$ propagation vector, corresponding to a specific order of planes with differing hole concentrations. The orderings on oxygen atoms are not experimentally dissociated from the orderings on the Mn atoms, in both compound, emphasizing the hybridized nature of the orbitals near ε_f.

Quantification of the hole densities, and of the $2p-3d$ hybridization, are foreseeable but will require *ab initio* calculations of both the ground states and the excited states, using dedicated formalisms, as the excited state corresponds to an electronic structure, with a strong Coulomb potential in a core shell, and an extra electron in the valence shell. Finally, as the RXD technique can also be chemically-sensitive to the magnetic moment, our results clearly suggest potential measurements of magnetic superstructures on the oxygen atoms. The RXD data open a new window on the $2p-3d$ states, the magnetic exchange couplings between $3d$ metals and on the electronic superstructures at play in this strongly correlated manganite system.

The data were taken at the Swiss Light Source of the Paul Sherrer Institut, where we benefitted from the support of the beamline staff on X11MA-SLS. Work performed at BNL was supported by US Dept of Energy, Division of Materials Science, under contract No. DE-AC02-98CH10886. We thank J. Debray of the Institut Néel for his excellent technical helps.

* Department of Physics, Pusan National University, Pusan 609-735, Korea

[1] J. M. Tranquada, B. J. Sternlieb, J. D. Axe, Y. Nakamura, and S. Uchida, Nature **375**, 561 (1995).
[2] T. Chatterji, ed., *Colossal Magnetoresistive Manganites* (Kluwer, Dordrecht, 2004).
[3] A. Rusydi, P. Abbamonte, H. Eisaki, Y. Fujimaki, G. Blumberg, S. Uchida, and G. A. Sawatzky, Phys. Rev. Lett. **97**, 016403 (2006).
[4] M. Abbate, F. M. F. de Groot, J. C. Fuggle, A. Fujimori, O. Strebel, F. Lopez, M. Domke, G. Kaindl, G. A. Sawatzky, M. Takano, et al., Phys. Rev. B **46**, 4511 (1992).
[5] G. Subías, J. García, M. G. Proietti, and J. Blasco, Phys. Rev. B **56**, 8183 (1997).
[6] A. Daoud-Aladine, J. Rodríguez-Carvajal, L. Pinsard-Gaudart, M. Fernández-Díaz, and A. Revcoleshi, Phys. Rev. Lett. **89**, 097205 (2002).
[7] V. Ferrari, M. Towler, and P. B. Littlewood, Phys. Rev.

Lett. **91**, 227202 (2003).
[8] D. V. Efremov, J. van den Brink, and D. I. Khomskii, Nature Materials **3**, 853 (2004).
[9] D. Volja, W.-G. Yin, and W. Ku, cond-mat:0704.1834v1 (2007).
[10] S. Grenier, V. Kiryukhin, S.-W. Cheong, B. G. Kim, J. P. Hill, K. J. Thomas, J. M. Tonnerre, Y. Joly, U. Staub, and V. Scagnoli, Phys. Rev. B **75**, 085101 (2007).
[11] J. Geck, P. Wochner, D. Bruns, B. Buchner, U. Gebhardt, S. Kiele, P. Reutler, and A. Revcolevschi, Phys. Rev. B **69**, 104413 (2004).
[12] N. Jaouen, J.-M. Tonnerre, G. Kapoujian, P. Taunier, J.-P. Roux, D. Raoux, and F. Sirotti, Journal of Synchrotron Radiation **11**, 363 (2004).
[13] *Resonant Anomalous X-Ray Scattering, Theory and Applications* (Materlik, Sparks and Fisher, 1994).
[14] H. L. Ju, H.-C. Sohn, and K. M. Krishnan, Phys. Rev. Lett. **79**, 3230 (1997).
[15] J. García, M. C. Sánchez, J. Blasco, G. Subías, and M. G. Proietti, J.Phys. Cond. Matt. **13**, 3243 (2001).
[16] S. Grenier, J. P. Hill, D. Gibbs, J. K. Thomas, M. v. Zimmermann, C. S. Nelson, Y. Tokura, Y. Tomioka, D. Casa, T. Gog, et al., Phys. Rev. B **69**, 134419 (2004).
[17] W.-G. Yin, D. Volja, and W. Ku, Phys. Rev. Lett. **96**, 116405 (2006).
[18] Y. Yamada, O. Hino, S. Nohdo, R. Kanao, T. Inami, and S. Katano, Phys. Rev. Lett. **77**, 904 (1996).
[19] M. Korotin, T. Fujiwara, and V. Anisimov, Phys. Rev. B **62**, 5696 (2000).